Electrical behaviors for growth of LAST alloys using vapor phase deposition

Mu-Li Chang*, Ming-Shan Jeng, Ya-Wen Chou, Jie-Ren Ku, Bin-Hao Chen

Industrial Technology Research Institute, Energy and Environment Laboratories, C600, Rm. 511, No. 8, Gongyan Rd., Liujia Shiang, Tainan County 734, Taiwan, ROC

ARTICLE INFO

ABSTRACT

The well-dispersed crystal structures of LAST (Lead Antimony Silver Tellurium) alloys grown by a vapor phase deposition method are demonstrated to have excellent electrical characteristics in this study. The atomic ratio of Pb to Te in the alloys are kept at 0.85–0.88. The distribution of component concentrations depends on the deposition temperature, and the Ag- and Sb-rich segments are fabricated at high deposition temperature. Experimental data suggest that the higher Sb content in the crystal increases carrier concentration up to $\sim 10^{19}$ (per cm). The electrical behavior of the crystal is n-type under Sb doping, and it was transferred into p-type once the samples are dominated by Ag doping, which also raises the mobility to a level as high as $\sim 10^3$ cm^2/V. Test results of this study have indicated that both Ag and Sb elements contribute to the electrical conductivity enhancement, however, an excess amount of Ag may significantly deteriorate the electrical performance instead.

1. Introduction

The effectiveness of thermoelectric material is related to dimensionless materials figure of merit, the so-called ZT value, defined by $ZT = S^2\sigma T/\kappa$, where S is the Seebeck coefficient (thermal power), σ the electrical conductivity, T the absolute temperature and κ the thermal conductivity [1]. Good thermoelectric materials require high electrical conductivity, high Seebeck coefficient, and low thermal conductivity, which are contrary requirements and have hindered the development of high performance thermoelectric materials for many years. Researches for better TE materials have recently accelerated due to many new multi-component alloys adopting new structure types and advanced processing technique [2–6]. LAST (Lead Antimony Silver Tellurium) alloys show high thermoelectric performance due to their nanodot effects [7]. However, the preparation of a multi-component alloy such as LAST is difficult and often leads to unrepeatable and inconsistent results among different research groups. One of the reasons for such inconsistency is the large difference of melting points between Ag and other elements in LAST alloys. The difference also results in composition segregation and distinct microstructure even in the same batch of samples [8,9].

Regarding LAST alloys manufacturing, Ao et al. reported that nano-sized AgPb$_{18}$SbTe$_{20}$ had been successful synthesized by hydrothermal method [10], and their powders consisted of spherical-shaped particles and rod-shaped particles. Wang, et al. demonstrated that Ag$_{0.8}$Pb$_{22}$SbTe$_{20}$ sample was prepared using a combined of mechanical alloying and spark plasma sintering with a maximum ZT = 1.37 [11]. Cai et al. reported that wet milling of LAST powers produced smaller particle and a fine powder particle size can enhance mechanical integrity of thermoelectric materials [12].

To achieve buck LAST alloys possessing homogeneous and well-dispersed micro/nano structures, we proposed growing LAST alloys in a vacuum environment using the vapor phase deposition method that had been successfully synthesizing PbSnTe single crystal with homogeneous structures [13]. Our preliminary results showed that defectiveness of microstructure formation is reduced and homogeneous LAST alloys are obtained. In this study, the feasibility of growing LAST alloys by vapor phase deposition was also discussed.

2. Experimental details

High purity element powders were well mixed in a proportion of AgSbPb$_{18}$Te$_{20}$. A contrast sample was first prepared by a conventional melting process as following. The powder mixture was sealed in a quartz tube under a vacuum of less than 10^{-4} torr and heated at 900 °C for 4 h. The temperature was then decreased to room temperature at a rate of 10 °C/h, which was changed to 20 °C/h as the temperature down to 450 °C. The obtained LAST sample from the above process was prepared and cleaned for the source of vapor phase deposition. The related vapor phase methods for growing crystal have been reported extensively [14].

A schematic diagram of crystal growth by vapor phase deposition method is shown in Fig. 1. The prepared melting process sample as the feeding source was placed at the bottom of a quartz tube having an inner diameter of 13 mm and a PbTe crystal as the seed was mounted at the bottom of a graphite rod with 12 mm diameter centrally located at the top of the quartz tube. The entire procedure must cautiously handle in order to avoid contact with any tube surface. The tube was sealed in a quartz tube under a vacuum of less than 10^{-4} torr. During the heating process, a rate of 20 °C was kept until the deposition temperature it reached. Then the temperature was lasted until the crystal grew. The ingot grown by this method exhibits composition variation along the growth direction and allows us to investigate the effects of compositional change on LAST alloy. The final ingots were sliced
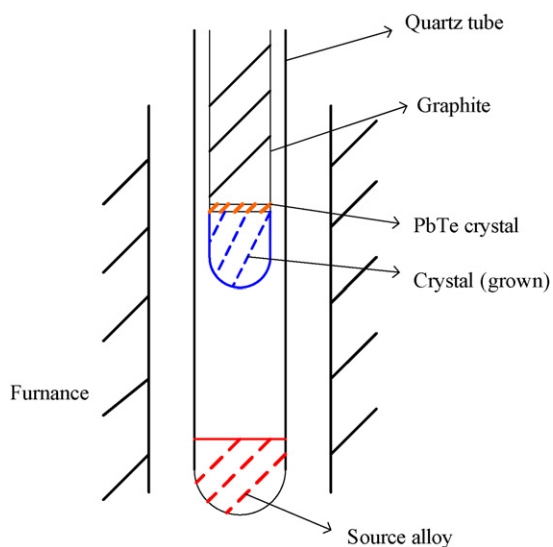

Fig. 1. Schematic diagram of the experimental set-up.

using diamond saw for measurement and analysis. The morphology and microstructure were analyzed by scanning electron microscopy (JEOL, JSM-5610). The electrical properties were measured by Hall Effect measurement system (ECOPIA, HMS-3000) at room temperature.

3. Results and discussion

The inhomogeneous structure of the melting process sample results from SEM analysis is shown in Fig. 2. The electrical properties are measured as 543 (per Ω/cm), 3.3×10^{18} (per cm^3), and 1000 (cm^2/Vs), respectively. Fig. 3 depicts the processing temperature profile of vapor phase deposition, which has a growth rate of 3.2 mm/day. The final ingot is a cylinder with 12 mm diameter and 24 mm length, see Fig. 4. The symmetric shape of the ingot is a result of symmetrical thermal flow during the deposition process, and the liquid droplets on the ingot top are formed due to vapor–liquid–solid mechanism [15,16].

The SEM picture and Ag element mapping of the melting process sample in Fig. 2 clearly show micro-scale Ag-rich regions, indicating that the Ag element is difficult to dissolve into LAST crystal using conventional melting method. Significant improvement by vapor phase deposition in the uniformity and the dispersion of Ag-rich
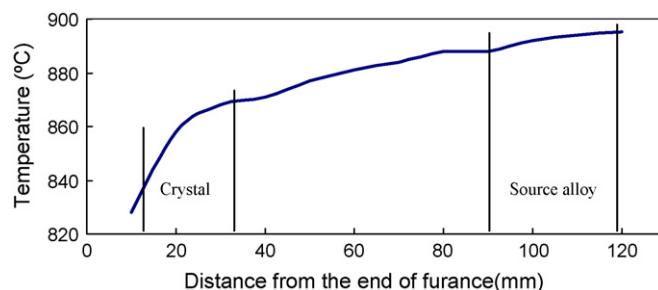

Fig. 3. Schematic diagram of the temperature for vapor phase deposition.

Fig. 4. The LAST alloys were grown using vapor phase deposition.

microstructure is shown in Fig. 5. The atomic ratio of Pb to Te does not change much along the growth direction as shown in Fig. 6. As rising deposition temperature, the deposition amount of Sb was increased and Ag element can only be found at higher temperature region in Fig. 7. No appearance of Ag at the initial stage resulted from the silver element having lower vapor pressure, shorter diffusion distance and the small portion of Sb and Ag within the source alloy. However, when the crystal kept growing and the deposition location was shifted to the higher temperature region, the residual of Ag in the source alloy was increased that were also helpful for the silver element deposition. It can be observed that 60.6 atomic % of Ag was found in the rest accumulation and deposition amount of Ag increased as well.
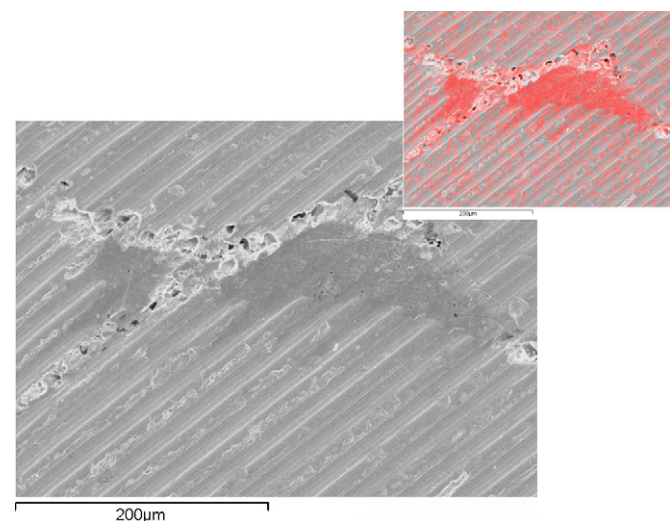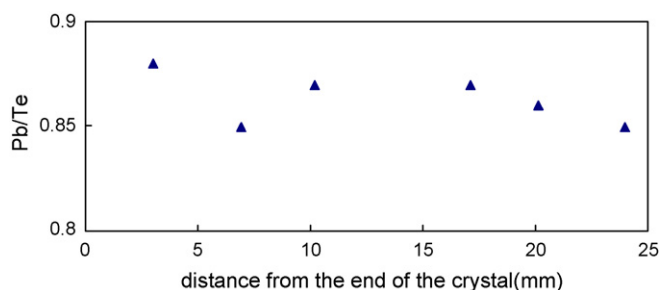

Fig. 2. SEM image of inhomogeneous LAST alloys structure and Ag mapping.
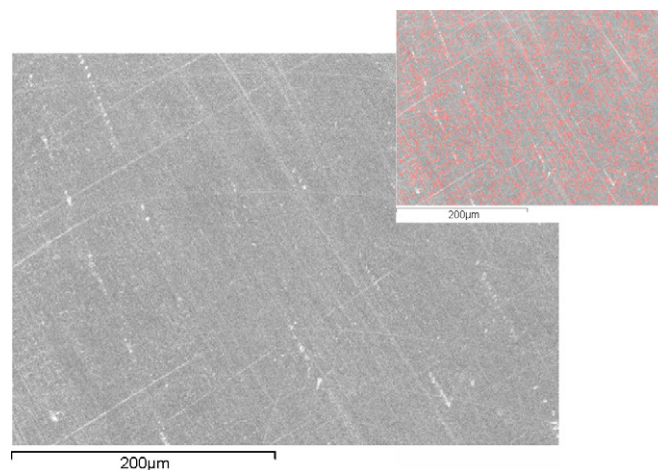
Fig. 5. SEM image of homogeneous LAST alloys structure and Ag mapping.

Fig. 6. Rate of Pb/Te in the crystal along the growth direction.
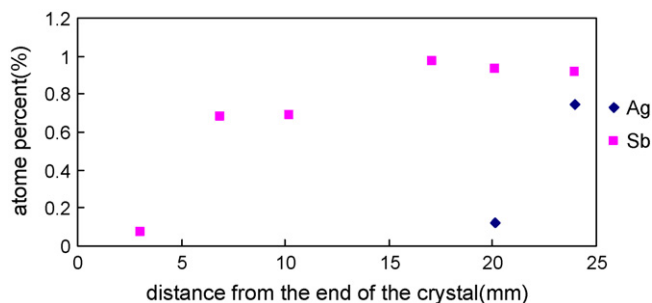
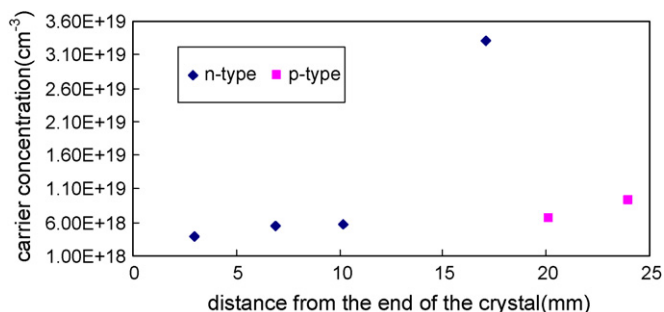**Fig. 7.** Distribution of Ag and Sb in the crystal along the growth direction.

Fig. 8. Carrier concentration vs different positions of the crystal.

Fig. 10. Electrical conductiivy vs different positions of the crystal.

the mobility significantly, while further increment of Ag content deteriorates the mobility.

Electrical conductivity distribution is shown in Fig. 10. The electrical conductivity was improved as the Sb content increased. It was apparently became higher associated with silver element, while an optimal Ag content for the maximum electrical conductivity exists. As a result, silver element plays a major role for the electrical behavior of the LAST alloys.

4. Conclusions

In this work, a phase vapor deposition method for manufacturing LAST alloy is demonstrated. In order to obtain bulk crystal with Ag structure, the deposition temperature must be kept as high as possible, and the amount of Ag in the source must be moderately increased. The distribution and concentration of Ag element have significant effects on LAST alloy's electrical behaviors. Even a small amount of Ag can improve the electrical properties significantly, it is important to precisely control the Ag concentration to achieve the best results. The technique developed in this work shows the potential of significantly enhancing the thermoelectric performance of LAST alloy. It is worth further exploring the possibility of improving the technique for manufacturing homogeneous LAST alloys with well-dispersed micro-structure.

Acknowledgements

Fig. 8 shows the carrier concentrations determined by Hall measurement. A high Sb content in the crystal is contributive to carrier concentrations. The samples measured in this study are n-type when Sb doping dominates and become p-type once Ag doping effect prevail. Note that previous studies have pointed out that Sb-doped PbTe materials are mainly n-type, and Ag doping possessed noticeable amphoteric behavior and is equally effective as a donor and an acceptor [17].

Fig. 9 shows the mobility of the samples higher Sb content does not obviously affect the mobility. However, the mobility is very sensitive to Ag content. Adding a small amount of Ag improves
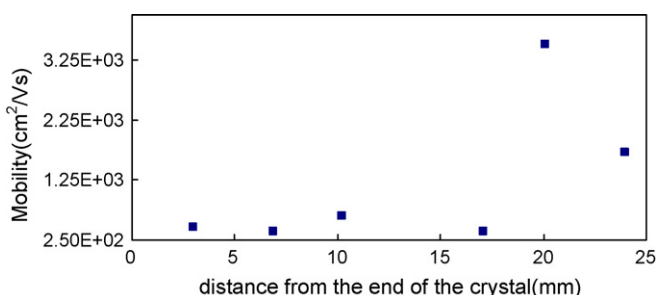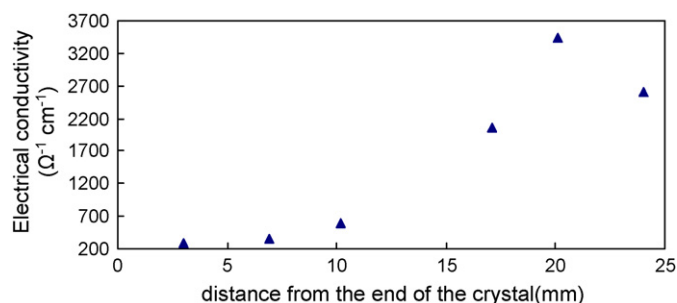
Fig. 9. Mobility vs different positions of the crystal.

References

[1] G.S. Nolas, J.W. Sharp, H.J. Goldsmid, Thermoelectrics: Basic Principles and New Materials Developments, Springer-Verlag, Heidelberg, 2001, pp. 10.
[2] F.J. DiSalvo, Science 285 (1999) 703.
[3] N. Soheilnia, J. Giraldi, A. Assoud, H. Zhang, T.M. Tritt, H. Kleinke, J. Alloys Compd. 448 (2008) 148.
[5] X. Tang, J. He, K. Aaron, E. Abbott, J.K. Kolis, T.M. Tritt, J. Cryst. Growth 310 (2008) 665.
[6] R. Venkatasubramanian, E. Siivola, T. Colpitts, B. O'Quinn, Nature 413 (2001) 597.
[7] K.F. Hsu, S. Loo, F. Guo, W. Chen, J.S. Dyck, C. Uher, T. Hogan, E.K. Polychroniadis, M.G. Kanatzidis, Science 303 (2004) 818.
[8] G.J. Snyder, N. Chen, F. Gascoin, E. Muller, G. Karpinski, C. Stiewe, Appl. Phys. Lett. 87 (2005) 171903.
[9] I.U. Arachchige, J. Wu, V.P. Dravid, M.G. Kanatzidis, Adv. Mater. 20 (2008) 3638.
[10] W.Q. Ao, W.A. Sun, J.Q. Li, F.S. Liu, Y. Du, J. Alloys Compd. 475 (2009) L22.
[11] H. Wang, J.F. Li, C.W. Nan, M. Zhou, Appl. Phys. Lett. 88 (2006) 092104.
[12] K.F. Cai, C. Yan, Z.M. He, J.L. Cui, C. Stiewe, E. Muller, H. Li, J. Alloys Compd. 469 (2009) 499.
[13] Z. Golacki, Z. Furmanik, M. Gorska, A. Szczerbakow, W. Zahorowski, J. Cryst. Growth 60 (1982) 150.
[14] R.K. Pandey, Solid State Commun. 15 (1974) 449.
[15] N. Tamari, H. Shtrikman, J. Electron. Mater. 8 (1979) 269.
[16] T.V. Saunina, D.B. Chesnokova, D.A. Jaskov, J. Cryst. Growth 71 (1985) 75.
[17] A.J. Strauss, J. Electron. Mater. 2 (1973) 553.